Received: 9 April 2021 | Revised: 14 September 2021 | Accepted: 14 September 2021

DOI: 10.1111/mmi.14813

RESEARCH ARTICLE

WILEY

Identification of Gip as a novel phage-encoded gyrase inhibitor protein of *Corynebacterium glutamicum*

Larissa Kever[1] | Max Hünnefeld[1] | Jannis Brehm[2] | Ralf Heermann[2] | Julia Frunzke[1]

[1]Institute of Bio- und Geosciences, IBG-1: Biotechnology, Forschungszentrum Jülich, Jülich, Germany

[2]Institut für Molekulare Physiologie, Biozentrum II, Mikrobiologie und Weinforschung, Johannes-Gutenberg-Universität Mainz, Mainz, Germany

Correspondence
Julia Frunzke, Institute of Bio- und Geosciences, IBG-1: Biotechnology, Forschungszentrum Jülich, 52425 Jülich, Germany.
Email: j.frunzke@fz-juelich.de

Funding information
H2020 European Research Council, Grant/Award Number: 757563; Helmholtz-Gemeinschaft, Grant/Award Number: W2/W3-096

Abstract

By targeting key regulatory hubs of their host, bacteriophages represent a powerful source for the identification of novel antimicrobial proteins. Here, a screening of small cytoplasmic proteins encoded by the CGP3 prophage of *Corynebacterium glutamicum* resulted in the identification of the *g*yrase-*i*nhibiting *p*rotein Cg1978, termed Gip. Pull-down assays and surface plasmon resonance revealed a direct interaction of Gip with the gyrase subunit A (GyrA). The inhibitory activity of Gip was shown to be specific to the DNA gyrase of its bacterial host *C. glutamicum*. Overproduction of Gip in *C. glutamicum* resulted in a severe growth defect as well as an induction of the SOS response. Furthermore, reporter assays revealed an RecA-independent induction of the cryptic CGP3 prophage, most likely caused by topological alterations. Overexpression of *gip* was counteracted by an increased expression of *gyrAB* and a reduction of *topA* expression at the same time, reflecting the homeostatic control of DNA topology. We postulate that the prophage-encoded Gip protein plays a role in modulating gyrase activity to enable efficient phage DNA replication. A detailed elucidation of the mechanism of action will provide novel directions for the design of drugs targeting DNA gyrase.

KEYWORDS

bacteriophages, DNA gyrase, gyrase inhibitors, prophage induction, topoisomerase II inhibitors

1 | INTRODUCTION

Bacteriophages represent the "dark matter" of the biological world (Hatfull, 2015; Ofir & Sorek, 2018; Rohwer & Youle, 2011). With the recent massive expansion of the genomic sequence space, the number of functionally unknown open reading frames (ORFs) in phage genomes is continuously increasing (Yin & Fischer, 2008). By targeting diverse cellular processes and regulatory hubs in their host cell, bacteriophages represent a rich source for the identification of novel antibacterial proteins as well as for the establishment of highly efficient molecular tools (De Smet et al., 2017; Nobrega et al., 2018; Roach & Donovan, 2015; Schroven et al., 2021). Especially, small cytoplasmic phage proteins have been shown to influence and reprogram a variety of key cellular processes, including transcription, translation, cell division, and central metabolism (De Smet et al., 2017; Orr et al., 2020; Storz et al., 2014).

DNA gyrase represents a type IIA topoisomerase present in all bacteria and plays a crucial role in the homeostatic control of DNA topology. Because of its unique ability to introduce negative supercoils into covalently linked double-stranded DNA (dsDNA), the

activity of DNA gyrase is indispensable for bacterial growth and a key target of antibacterial agents. The heterotetrameric enzyme consists of two GyrA and two GyrB subunits ($GyrA_2GyrB_2$). While the GyrA subunit of the enzyme catalyzes the breakage and resealing of dsDNA, the GyrB subunit exhibits ATPase activity (Bush et al., 2015; McKie et al., 2021; Vanden Broeck et al., 2019). Currently, two major classes of small molecule drugs targeting the bacterial gyrase are known: the aminocoumarins and the quinolones (Collin et al., 2011). Besides a range of small molecules, also some proteinaceous, bacterial toxins were found to inhibit the activity of the gyrase, including Microcin B17 (Pierrat & Maxwell, 2003), a glycine-rich peptide found in *Escherichia coli* strains carrying the *mcb* operon as well as the CcdB toxin as part of the *ccd* toxin–antitoxin system encoded by the F-plasmid (Dao-Thi et al., 2005; Miki et al., 1992).

Corynebacterium glutamicum—a member of the phylum Actinobacteria—is an important industrial platform organism used for the industrial production of a wide range of value-added compounds, including amino acids, organic acids, and proteins (Wendisch et al., 2016). The genome of the model organism *C. glutamicum* ATCC 13032 contains four cryptic prophages (CGP1-4) (Frunzke et al., 2008; Ikeda & Nakagawa, 2003). The largest prophage CGP3 (~219 kb, containing also prophage CGP4) was shown to be inducible in an SOS-dependent manner as well as in an SOS-independent manner (Helfrich et al., 2015; Nanda et al., 2014; Pfeifer et al., 2016). Recently, the Lsr2-type protein CgpS was identified as a prophage-encoded nucleoid-associated protein involved in the silencing of phage gene expression maintaining the lysogenic state of the large CGP3 prophage (Pfeifer et al., 2016). Interference with CgpS binding was shown to result in prophage activation and consequently cell death.

In this study, a systematic screening of small cytoplasmic proteins encoded by the CGP3 prophage of *C. glutamicum* resulted in the identification of phage proteins causing severe growth defects and prophage induction. The small phagic protein Cg1978 was further shown to directly target the DNA gyrase enzyme by interacting with the GyrA subunit and inhibiting the supercoiling activity of the *C. glutamicum* DNA gyrase in vitro. Cg1978 was therefore termed Gip for *g*yrase *i*nhibiting *p*rotein. A detailed elucidation of the mechanism of action may point to novel directions for the design of drugs targeting DNA gyrase.

2 | RESULTS

2.1 | Systematic screening of small CGP3-encoded proteins influencing growth and prophage induction

Most of the proteins encoded by the cryptic CGP3 prophage are of unknown function. Phage proteins were shown to frequently target key regulatory hubs to shut down bacterial metabolism (Roach & Donovan, 2015). In this study, we screened the impact of overall 11 small (<75 amino acids), cytoplasmic phage-encoded proteins on cellular growth and prophage induction. For this purpose, plasmid-based overexpression (pAN6-*GOI*) of the selected genes of interest was performed in the prophage reporter strain *C. glutamicum* ATCC 13032::P_{lys}-*eyfp*. In previous studies, this chromosomal reporter (P_{lys}-*eyfp*) was successfully established to translate prophage activation into a fluorescent output (Helfrich et al., 2015). During cultivation, biomass was measured as a function of backscattered light intensity with an excitation wavelength of 620 nm. Following this approach, the overproduction of 9 out of 11 phage proteins (Cg1902, Cg1910, Cg1924, Cg1925, Cg1971, Cg2026, Cg2035, Cg2045, and Cg2046) displayed comparable phenotypes as the empty vector control regarding backscatter signal and fluorescence output measured via flow cytometry (Figure 1c and Figure S1a,b). By contrast, overproduction of Cg1914 and Cg1978 showed a significant effect on growth and prophage induction in the presence of 50 μM IPTG. Cg1914 overproduction resulted in a reduced growth rate ($\mu = 0.23 \pm 0.01\ hr^{-1}$) and a reduced final backscatter (Figure 1a, *blue line*) compared with the empty vector control pAN6 ($\mu = 0.38 \pm 0.01\ hr^{-1}$). In the case of Cg1978, overproduction led to an elongated lag-phase, but the final backscatter as well as the growth rate in the exponential phase ($\mu = 0.36 \pm 0.01\ hr^{-1}$) (Figure 1a, *red line*) were comparable with those of the empty vector control.

A comparable impact on cell growth due to cg1914 or cg1978 overexpression was also detected in the prophage-free strain MB001, indicating that the observed growth defect was independent of the presence and/or activity of the CGP3 island (Figure 1b).

For both target proteins, Cg1914 and Cg1978, overproduction resulted in an increased fluorescence signal after 24 hr of cultivation (cg1914: 7.4 ± 2.6% induced cells, cg1978: 3.5 ± 0.2% induced cells) indicating CGP3 prophage induction in the respective subpopulation (Figure 1c). As a positive control, we expressed an N-terminally truncated variant of the prophage silencer CgpS (CgpS-N), which was previously shown to trigger prophage induction (Pfeifer et al., 2016).

Since overproduction of Cg1914 and Cg1978 showed a high impact on prophage induction, we tested the inducibility of the CGP3 prophage in mutants lacking the respective genes using a plasmid-based prophage reporter (P_{lys}-*lys´-venus*). Remarkably, the corresponding strains *C. glutamicum* ATCC 13032 Δcg1914 and Δcg1978 featured no difference—neither in cell growth nor in prophage inducibility—upon treatment with the DNA-damaging antibiotic mitomycin C (Tomasz, 1995), which was used to trigger SOS-dependent prophage induction (Figure S2). These results indicated that both proteins are not essentially involved in SOS-dependent CGP3 induction. Prophage induction, therefore, appeared to be an indirect effect of Cg1914 or Cg1978 overproduction. Based on further results described in the following, we focused on the role and cellular target of the small phage protein Cg1978.

2.2 | Overproduction of Cg1978 triggers the activation of SOS response and RecA-independent prophage induction

As the CGP3 prophage was already characterized to be inducible in an SOS-dependent manner as well as in an SOS-independent

manner (Helfrich et al., 2015; Nanda et al., 2014; Pfeifer et al., 2016), we determined the SOS dependency of Cg1978-mediated prophage induction. To this end, the fluorescent outputs of different reporter strains were measured via flow cytometry in a time-resolved manner during cg1978 overexpression. Besides the prophage reporter strain (*C.g.* ATCC 13032::P_{lys}-*eyfp*), an SOS reporter strain (*C.g.* ATCC 13032::P_{recA}-*venus*) as well as an SOS-deficient prophage reporter strain (*C.g.* ATCC 13032 Δ*recA*::P_{lys}-*eyfp*) lacking the coprotease RecA—required for the induction of the host SOS response (Janion, 2008)—were used.

As described above, overexpression of cg1978 resulted in a similar growth phenotype of all reporter strains characterized by an elongated lag-phase (marked in gray) with subsequent wild type-like growth (Figure 2a). The impaired cell growth under cg1978 overexpression conditions was confirmed by time-lapse fluorescent microscopy of a *C. glutamicum* microcolony of the prophage reporter strain, which was grown in a microfluidic chamber. Increased levels of Cg1978 led to elongated cell morphology and a small fraction of cells featuring a strongly increased output of the prophage reporter (Figure 2c and Videos S1 and S2).

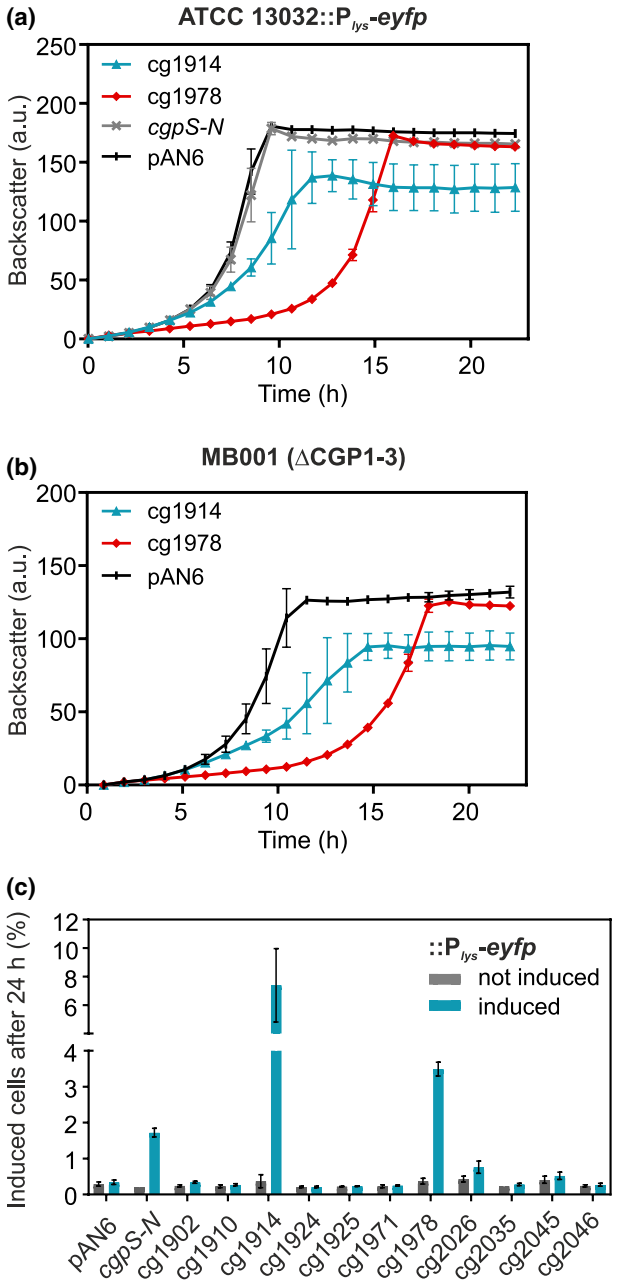

FIGURE 1 Screening of small phagic proteins regarding their impact on cellular growth and CGP3 induction in *Corynebacterium glutamicum*. The cultivation of the prophage-reporter strain *C. glutamicum* ATCC 13032::P_{lys}-*eyfp* and the prophage-free strain MB001 carrying the corresponding gene sequences of the small proteins on the pAN6 vector (under control of P_{tac}) was performed in CGXII-Kan_{25} medium with 2% (w/v) glucose and 50 μM IPTG for 24 hr. All data represent mean values with standard deviations from three independent biological replicates ($n = 3$). (a) Growth curves of the prophage reporter strain (*C. glutamicum* ATCC 13032::P_{lys}-*eyfp*) upon small protein overproduction are based on the backscatter measurements in the BioLector® microcultivation system. (b) Growth curves of the prophage-free strain MB001 upon small protein overproduction are based on the backscatter measurements in the BioLector® microcultivation system. (c) Percentage of induced cells after 24 hr cultivation without and with 50 μM IPTG based on the flow cytometric measurements of the prophage reporter strain *C. glutamicum* ATCC 13032::P_{lys}-*eyfp*

Measurement of the reporter output over time not only confirmed CGP3 induction but also revealed an induction of the cellular SOS response (Figure 2b). Interestingly, the wild type-like and the RecA-deficient prophage reporter strain showed nearly the same percentage of induced cells upon cg1978 overexpression throughout the entire measurement, reaching a peak value after 9.5 hr of cultivation (Δ*recA*::P_{lys}-*eyfp*: 4.6 ± 0.7, P_{lys}-*eyfp*: 4.8 ± 0.9). These results emphasize RecA-independent CGP3 induction as an indirect effect of cg1978 overexpression.

Remarkably, all reporter strains revealed an increasing fluorescence during the lag-phase, which decreased again upon transition into the exponential growth phase (Figure 2b), suggesting the growth of a subpopulation resistant to Cg1978 overproduction effects.

2.3 | Cg1978 directly interacts with gyrase subunit A (GyrA)

To identify the direct cellular target of Cg1978, we performed an in vitro pull-down assay. For this purpose, the small protein Cg1978 containing a C-terminal Strep-tag was overproduced in *E. coli* BL21 (DE3) and purified via affinity purification. The purified target protein was incubated with *C. glutamicum* cell extract and this sample was again passed over a Strep-Tactin column to identify proteins copurifying with Cg1978. SDS-PAGE analysis of proteins coeluting with Cg1978 revealed an additional protein band at ~100 kDa (Figure 3a). Analysis of the copurified protein via MALDI-TOF as well as LC-MS/MS analysis of the whole elution fraction indicated the copurification of Cg1978 with *C. glutamicum (C.g.)* DNA gyrase subunit A (~95 kDa), a subunit of the heterotetrameric ATP-dependent DNA gyrase complex (A_2B_2). The DNA gyrase belongs

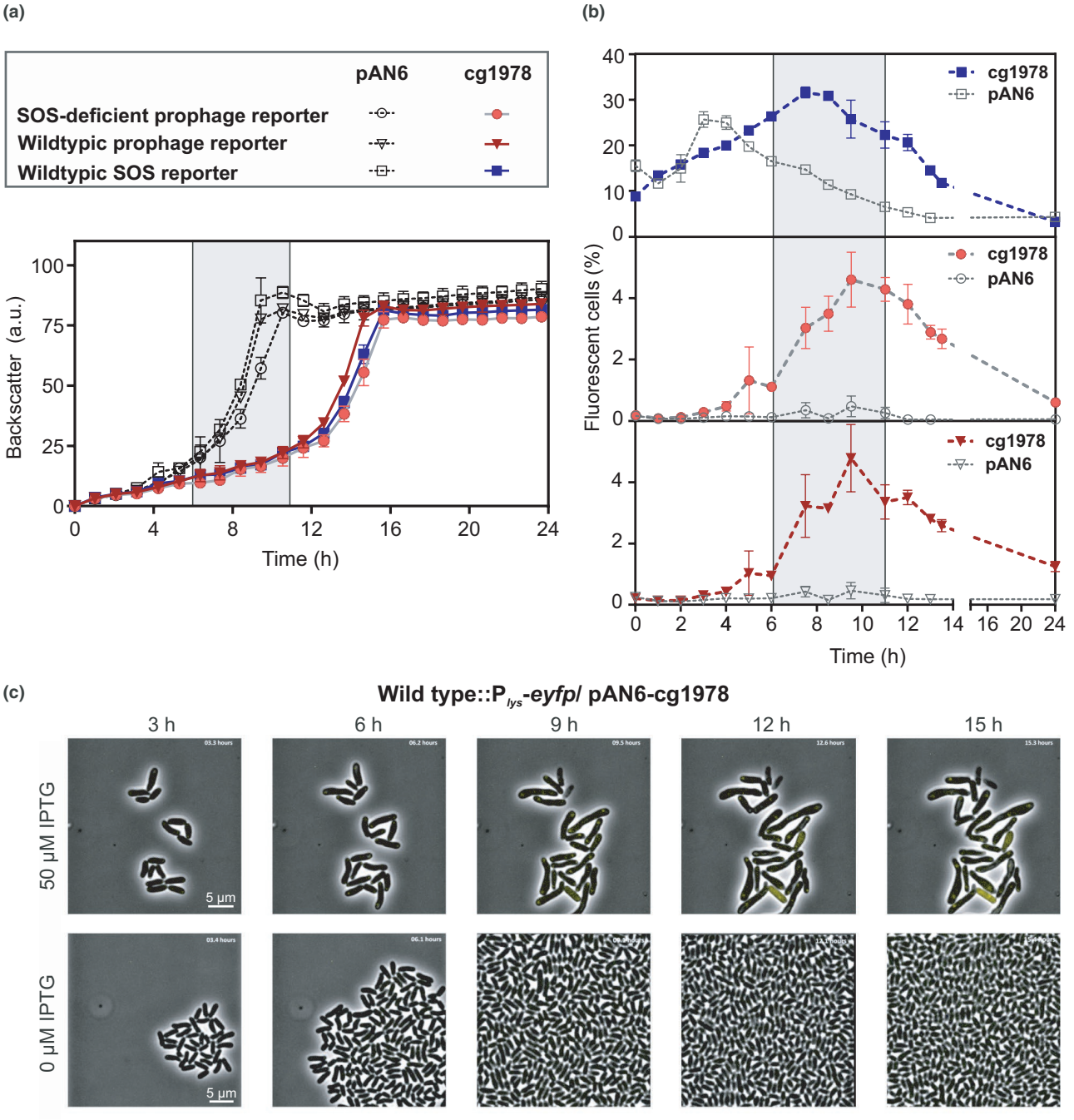

FIGURE 2 Time-resolved measurement of reporter outputs upon Cg1978 overproduction in *Corynebacterium glutamicum* showed activation of SOS response and RecA-independent prophage induction. Cultivation of an SOS reporter strain ATCC 13032::P_{recA}-*venus*, a prophage reporter strain ATCC 13032::P_{lys}-*eyfp* and an SOS-deficient prophage reporter strain ATCC 13032 Δ*recA*::P_{lys}-*eyfp* carrying the plasmids pAN6 or pAN6-cg1978 was performed in the BioLector® microcultivation system in CGXII-Kan_{25} medium with 2% (w/v) glucose and 50 µM IPTG. All data represent mean values with SDs from three independent biological replicates ($n = 3$). (a) Growth curves based on the backscatter measurements in the BioLector® microcultivation system. The elongated lag-phase of the Cg1978 overproducing strain is marked in gray. (b) Percentage of induced cells based on the flow cytometric measurements of eYFP or Venus fluorescence of the reporter strains. (c) Time-lapse fluorescence imaging of the *C. glutamicum* prophage reporter strain ATCC 13032::P_{lys}-*eyfp* carrying the pAN6-cg1978 plasmid. Cells were cultivated in PDMS-based microfluidic chip devices (Grünberger et al., 2015) using CGXII-Kan_{25} medium with 2% (w/v) glucose. The medium was continuously supplied with a flow rate of 300 nl/min. Overexpression of cg1978 was induced by the addition of 50 µM IPTG. Fluorescent images represent cutouts from Videos S1 and S2

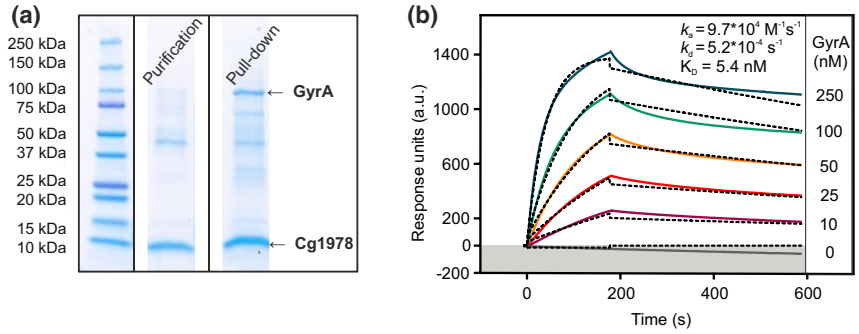

FIGURE 3 Cg1978 directly interacts with the gyrase subunit A (GyrA) in vitro. (a) The small protein Cg1978 containing a C-terminal Strep-tag was overproduced in *Escherichia coli* BL21 (DE3) and purified via affinity purification. For the pull-down assay, the *Corynebacterium glutamicum* wild-type strain was cultivated in BHI medium until OD_{600} of 6. The purified target protein was incubated with *C. glutamicum* cell extract and again passed over a Strep-Tactin column aiming at the copurification of Cg1978 with possible interaction partners. Proteins in the elution fractions were analyzed via SDS-PAGE using the Precision Plus Protein™ Dual protein marker as a standard and further identified using LC-MS/MS and MALDI-TOF. Gels were spliced for labeling purposes. (b) Surface plasmon resonance spectroscopy of GyrA-N-Strep binding to Cg1978-C-His (k_a, association constant; k_d, dissociation constant, K_D, equilibrium dissociation constant). The colored lines represent the experimental data, the dotted lines represent the fitted data using a 1:1 binding algorithm that was the basis for the binding kinetics calculation

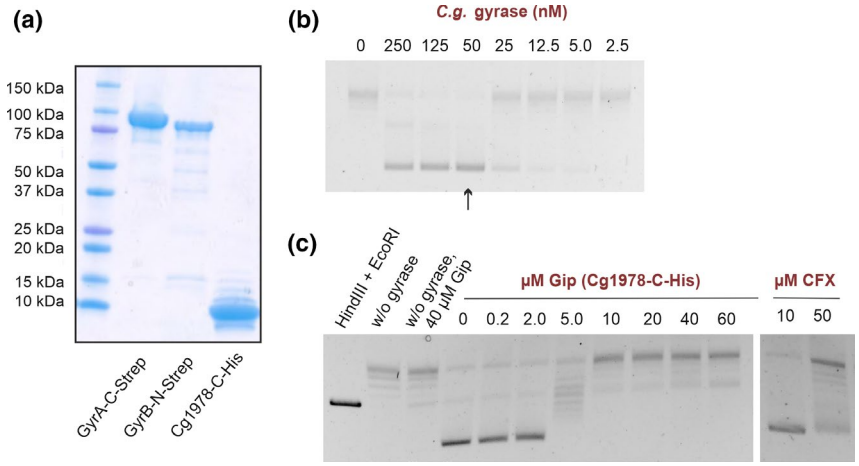

FIGURE 4 Cg1978 inhibits gyrase supercoiling activity in vitro. The assay was conducted according to the manual of the *Mycobacterium tuberculosis* Gyrase (HIS) Supercoiling Assay Kit from Inspiralis (Norwich, UK). (a) Cg1978 containing a C-terminal His-tag as well as gyrase subunit A containing a C-terminal and subunit B containing an N-terminal Strep-tag were separately overproduced in *Escherichia coli* BL21 (DE3) and purified via affinity purification. (b) After formation of the heterotetrameric gyrase complex, the activity assay of the purified DNA gyrase from *Corynebacterium glutamicum* ATCC 13032 was performed to identify the gyrase concentration required for maximal supercoiling of 0.5 µg relaxed plasmid DNA, which was defined as 1 U. (c) Supercoiling inhibition assay to test the inhibitory effect of Cg1978 on 1 U of the DNA gyrase from *C. glutamicum* ATCC 13032. Incubation of relaxed plasmid DNA with Cg1978 in the absence of DNA gyrase was used as a negative control to screen for any nuclease activity. The known gyrase inhibitor Ciprofloxacin (CFX) served as a positive control for efficient gyrase inhibition. Two agarose gels were compiled as indicated by the boundaries

to the subclass of type II topoisomerases and plays a key role in DNA metabolism as it is able to introduce negative supercoiling to double-stranded DNA in an ATP-dependent manner. Gyrase subunit B was also detected in the elution fraction, but in a significantly lower amount compared to GyrA rather suggesting unspecific copurification.

As a next step, surface plasmon resonance spectroscopy was used to examine the binding affinity of Cg1978 to GyrA. The sensorgram revealed a stable and specific 1:1 interaction between Cg1978 and GyrA with a high association rate (k_a = 9.7 × 10^4 M^{-1} s^{-1}) and a slow dissociation rate (k_d = 5.2 × 10^{-4} s^{-1}) resulting in an overall affinity (K_D) of 5.4 nM (Figure 3b). Purification of Cg1978-C-His and GyrA-N-Strep for SPR analysis are shown in Figure S3.

2.4 | Cg1978 inhibits DNA supercoiling via interaction with the DNA gyrase in vitro

Due to its essential role for cell survival, DNA gyrase represents an important drug target of antibiotics and protein-based inhibitors (Collin et al., 2011). Based on the observed growth defect upon Cg1978 overproduction and the interaction with GyrA, we

further assessed the effect of Cg1978 on gyrase activity by performing in vitro supercoiling inhibition assays with the purified enzyme.

For this purpose, Cg1978-C-His, GyrA-C-Strep, and GyrB-N-Strep from *C. glutamicum* were purified separately using affinity chromatography (Figure 4a). The formation of the heterotetrameric enzyme complex was obtained by incubating equimolar amounts of both gyrase subunits on ice for 30 min. In the first step, the activity of the purified *C.g.* DNA gyrase was measured by incubating 0.5 μg relaxed pBR322 plasmid DNA with different *C.g.* gyrase concentrations. The addition of increasing *C.g.* gyrase concentrations led to an increase in supercoiling of the plasmid DNA resulting in maximal supercoiling using 50 nM of *C.g.* gyrase. This concentration was defined as 1 U (corresponding to a specific activity of 1.88×10^3 U/mg) and was used for testing the potential inhibitory effect of Cg1978 (Figure 4b).

As shown in Figure 4c, incubation of increasing concentrations of Cg1978 (0.2–60 μM) with 1 U *C.g.* DNA gyrase and relaxed plasmid DNA resulted in a decreased supercoiling activity of the *C.g.* DNA gyrase. Complete inhibition of the introduction of supercoils by DNA gyrase was achieved by the addition of 10 μM Cg1978 leading to an accumulation of the relaxed/nicked conformation. Therefore, we named the gene product of cg1978 Gip (*g*yrase *i*nhibiting *p*rotein).

As a negative control, Gip was incubated with relaxed plasmid DNA in absence of DNA gyrase to visualize any potential nuclease activity in the elution fraction of Gip. A slight band reflecting linear DNA could be detected when adding 40 μM Gip. However, incubating increasing concentrations of Gip with the *C.g.* DNA gyrase did not lead to an accumulation of linear DNA. As a positive control, the known fluoroquinolone-based gyrase-inhibitor ciprofloxacin (CFX) stabilizing the gyrase-DNA cleavage complex (Drlica & Malik, 2003) was used showing significant inhibition of the supercoiling activity of the *C.g.* gyrase at 50 μM (16.6 μg/ml). This was in line with already published data for the DNA gyrase of *Mycobacterium smegmatis*, which showed 50% inhibition of the supercoiling activity of 1 U gyrase by the addition of 10 μg/ml CFX (Manjunatha et al., 2002). As for Gip, inhibition of the DNA gyrase via CFX led to an accumulation of the relaxed/nicked plasmid conformation.

To further investigate the activity profile of Gip, we determined its effect on the DNA gyrases of *Mycobacterium tuberculosis* and *E. coli*. Gyrase subunits A of the actinobacterial species *C. glutamicum* and *M. tuberculosis* (*M.tb.*) share a sequence identity of ~71%, while GyrA of *C. glutamicum* and *E. coli* (*E.c.*) only show a ~45% sequence identity (Figures S4 and S5). As described previously for the DNA gyrase of *C. glutamicum*, 1 U of the *E.c.* and *M.tb.* gyrases were used to examine supercoiling inhibition via Gip. The supercoiling assay showed no significant change in the supercoiling activity of the respective gyrases when adding increasing concentrations of Gip. In case of the *M.tb.* gyrase, a slight shift from supercoiled plasmid DNA to linear plasmid DNA could be detected by addition of 40 μM Gip, which was even less pronounced for the *E.c.* gyrase. The corresponding assays are shown in Figure S6.

2.5 | Compensatory expression of *gyrAB* and *topA* as a response to gyrase inhibition via Gip

Supercoiling inhibition assays showed that Cg1978 (Gip) is a gyrase-inhibiting protein. As the activity of DNA gyrase is indispensable for bacterial growth, we investigated the impact of *gip* overexpression on the transcriptome of *C. glutamicum*. Since the *gip* overexpressing strain revealed a wild type-like growth rate after an elongated lag-phase, we were especially interested to understand how the bacterial host counteracts gyrase inhibition. For this purpose, comparative transcriptome analysis of the *C. glutamicum* ATCC 13032 strain containing the empty vector control and the strain containing the overexpression plasmid pAN6-*gip* was performed using DNA microarrays. The shown transcriptomic changes are based on mRNA levels of cells harvested at an OD_{600} of 6 in the mid-exponential growth phase.

The *gip* overexpressing strain showed a partial upregulation of CGP3 genes due to overexpression of *gip* (Table S4), confirming the prophage induction also revealed by the above-described reporter assays. Apart from the CGP3 region, overexpression of *gip* led to upregulation of 352 genes and downregulation of 333 genes reflecting the high impact of gyrase inhibition on overall cell metabolism.

Interestingly, both gyrase subunits *gyrA* and *gyrB* were markedly upregulated showing a more than 4-fold increase in expression levels (Table 1). In contrast, *topA* coding for topoisomerase I, which catalyzes the opposing reaction of DNA gyrase by removing negative supercoils, showed a reduced expression level. Moreover, the expression of further genes involved in DNA metabolism was influenced by *gip* overexpression including for example the reduced expression of genes coding for helicases (exemplarily cg0838, cg0842, cg0843, cg0845, cg0889, and cg1498). Additionally, 10 targets of the SOS key player LexA, for example, *recN* (DNA repair) and *ftsK* (cell division and chromosome segregation), showed an increased mRNA ratio, which was in line with the high fluorescent outputs of the SOS reporter strain upon Gip overproduction (Table 1, see Table S4 for the complete list of genes with altered expression levels).

3 | DISCUSSION

In this study, a screening of small cytoplasmic proteins encoded by the CGP3 prophage of *C. glutamicum* resulted in the identification of the novel gyrase inhibitor protein Gip (Cg1978, 6.8 kDa). Overproduction of Gip resulted in significant growth defects and prophage induction in a subpopulation. Further characterization of this small phagic protein confirmed a specific, stable, and high-affinity interaction with the GyrA subunit and inhibition of the supercoiling activity of the DNA gyrase in vitro.

DNA gyrase possesses the unique ability to catalyze the ATP-dependent negative supercoiling of double-stranded DNA by cleaving and rejoining it (Bush et al., 2015). Supercoiling inhibition assays showed that Gip-mediated gyrase inhibition resulted in the accumulation of the nicked/relaxed plasmid conformation, while no more

TABLE 1 Impact of *gip* (cg1978) overexpression on global expression levels

Gene locus	Gene name	Annotation	mRNA ratio
Genes coding for proteins involved in DNA metabolism			
cg0015	*gyrA*	DNA gyrase subunit A, DNA topoisomerase II	6.23
cg0007	*gyrB*	DNA gyrase subunit B, DNA topoisomerase II	4.44
cg0373	*topA*	DNA topoisomerase I	0.40
cg0845		Putative superfamily II DNA/RNA helicase, SNF2 family	0.49
cg0889		Putative DNA helicase RecQ	0.48
cg0843		Putative helicase	0.45
cg1498		Putative RecG-like helicase	0.43
cg0842		Putative DNA helicase	0.39
cg0838		Putative helicase	0.22
LexA target genes			
cg1602	*recN*	DNA repair protein	10.96
cg1255		Putative HNH endonuclease, conserved	5.11
cg1977		Putative secreted protein	4.52
cg0470	*htaB*	Secreted heme transport-associated protein	4.41
cg0738	*dnaE2*	DNA polymerase III subunit α	3.11
cg1288		Putative multidrug efflux permease of the major facilitator superfamily	2.83
cg1080		Putative multicopper oxidase	2.67
cg2158	*ftsK*	Cell division protein	2.46
cg0713		Hypothetical protein	2.13
cg2114	*lexA*	Transcriptional regulator, involved in SOS/stress response	2.09
cg2950	*radA*	Putative ATP-dependent protease, DNA repair	0.48
cg2381		Hypothetical protein	0.47
cg0834	*tusE*	Bacterial extracellular solute-binding protein, trehalose uptake system	0.34
cg0841		Hypothetical protein	0.31
cg1314	*putP*	Proline transport system	0.30
cg3345		Hypothetical protein	0.24

Note: A genome-wide comparison of mRNA levels of the *Corynebacterium glutamicum* ATCC 13032 strain overexpressing *gip* and the wild-type strain carrying the empty vector control was performed. The shown mRNA ratios indicate mean values from three independent biological replicates ($n = 3$). The strains were cultivated in CGXII-Kan_{25} minimal medium with 2% (w/v) glucose and 50 μM IPTG and mRNA was prepared from cells harvested at an OD_{600} of 6. The mRNA ratios were calculated by dividing the mRNA levels of the *gip* overexpressing strain by the mRNA levels of the strain carrying the empty vector control. The table includes selected genes from a larger set which showed a changed mRNA level in all experiments (mRNA ratio >2.0: upregulation [red] or <0.5: downregulation [green], *p*-value <0.05).

supercoiled plasmid DNA was detectable (Figure 4). Different molecular mechanisms of gyrase inhibition have been described so far. Fluoroquinolones and the well-characterized proteinaceous bacterial toxins Microcin B17 (MccB17, 3.1 kDa) and CcdB (11.7 kDa) poison the DNA gyrase by stabilizing the gyrase-DNA cleavage complex leading to double-strand DNA breaks (Bernard et al., 1993; Drlica & Malik, 2003; Pierrat & Maxwell, 2003). In contrast, aminocoumarins (e.g. novobiocin) inhibit ATP hydrolysis as the binding site overlaps with the ATP-binding pocket of the GyrB subunit (Maxwell & Lawson, 2003). Further proteins targeting DNA gyrase are pentapeptide repeat proteins (PRPs) like Qnr proteins or MfpA, whose inhibitory interaction is proposed to be based on DNA mimicry (Shah & Heddle, 2014). However, no conserved domains of Gip with other known proteinaceous gyrase inhibitors could be identified using the

conserved domain database (CDD) with Reverse Position-Specific BLAST (RPS-BLAST) (Lu et al., 2020). Accordingly, further studies and structural analysis are required to elucidate the exact molecular mechanism of Gip-mediated gyrase inhibition.

Investigations regarding the activity profile of Gip suggested that the inhibitory activity seems to be highly specific for the DNA gyrase of its bacterial host *C. glutamicum*, as the DNA gyrase of *M. tuberculosis* and *E. coli* were not significantly affected by Gip. Similar observations were made for the proteinaceous bacterial toxins Microcin B17 (MccB17, 3.1 kDa) and CcdB (11.7 kDa), which target the DNA gyrase of their host *E. coli* in vitro, while no inhibition of the DNA gyrase of *M. smegmatis* could be detected (Chatterji et al., 2001). Even though DNA gyrase is a conserved protein among bacteria, Gram-positive and Gram-negative bacteria show substantial differences in the amino acid sequence of GyrAB (Madhusudan & Nagaraja, 1996; Manjunatha et al., 2000). Accordingly, the absence of specific target residues potentially explains the different levels of susceptibility of the DNA gyrases to proteinaceous toxins (Chatterji et al., 2001).

Reporter outputs of the RecA-dependent SOS reporter strain and transcriptomic analysis of Gip overproducing cells revealed an induction of the SOS response (Figure 2b, Table 1). These findings are in agreement with already published data describing activation of the SOS response as one of the pleiotropic effects of gyrase inhibition (Jeong et al., 2006). Stabilization of the gyrase-cleaved DNA complex results in arrested replication forks and widespread DNA damage by stimulating the formation of DNA breaks triggering the SOS response (DeMarini & Lawrence, 1992; Dwyer et al., 2007).

Gip overproduction was further shown to activate the induction of the CGP3 prophage. However, the fact that the observed growth defect of Gip overproducing cells is independent of the presence of the CGP3 prophage (Figure 1b) and that deletion of *gip* did not result in altered inducibility of CGP3 (Figure S2) emphasize prophage activation as an indirect effect of Gip overproduction. Recent studies already confirmed that CGP3 is inducible in an SOS-dependent manner as well as in an SOS-independent manner (Helfrich et al., 2015; Nanda et al., 2014; Pfeifer et al., 2016). As the wild type and the RecA-deficient prophage reporter strain revealed nearly identical fluorescent outputs, we propose that prophage induction occurred mainly in a RecA-independent manner. Here, influencing the introduction of supercoils due to gyrase inhibition might be a possible reason for CGP3 induction. The lysogenic state of CGP3 is maintained by the Lsr2-type silencer protein CgpS, which was shown to target more than 35 AT-rich regions within the CGP3 element (Pfeifer et al., 2016). The formation of this dense nucleoprotein complex was shown to be crucial for efficient CgpS-mediated silencing (Wiechert et al., 2020). Especially in the case of proteins-targeting AT-rich DNA sequences, the topologic state of DNA can affect protein–DNA interactions (Dorman & Dorman, 2016). Apart from that, different studies already demonstrated an influence of DNA supercoiling on the λ repressor and the lysogenic-lytic decision of phage λ (Ding et al., 2014; Norregaard et al., 2013, 2014).

In general, it is conceivable that the CGP3 prophage could have an advantage from encoding a gyrase inhibitor as it might allow a more efficient phage DNA replication by modulating host gyrase activity. Similar assumptions were recently made for the topo I inhibitor protein gp55.2 encoded by the T4 phage of *E. coli*. It was hypothesized that modulating DNA relaxation activity of topo I is required for an optimal phage yield during infection (Mattenberger et al., 2015). Another example of a phage-encoded protein altering DNA topology is represented by the gyrase-inhibiting peptide Igy encoded by phage LUZ24 infecting *Pseudomonas aeruginosa* (De Smet et al., 2021). Interaction of Igy with GyrB, possibly by functioning as a DNA mimicry protein, inhibits the DNA gyrase and LUZ24 infection seems to be independent of a functioning host DNA gyrase.

Global topological alterations caused by Gip overproduction were also reflected by the transcriptome analysis revealing a marked impact on global gene expression patterns (Table 1). As DNA gyrase is indispensable for replication and transcription by changing the topological state of DNA, its inhibition was previously described to globally affect the gene expression profile (Guha et al., 2018; Jeong et al., 2006). Particularly noteworthy in this context are the significantly increased mRNA levels of *gyrA* and *gyrB* as well as the downregulation of *topA*. The DNA topology modulatory proteins, gyrase and topoisomerase I (topo I), catalyze opposing reactions of DNA supercoiling and relaxation (McKie et al., 2021). Previous studies already revealed that expression of the *gyrAB* and *topA* is controlled in a supercoiling-sensitive manner: While increasing DNA relaxation stimulates *gyrAB* expression (Menzel & Gellert, 1983), it represses expression of *topA* allowing homeostatic maintenance of DNA topology (Ahmed et al., 2016; Tse-Dinh, 1985). As gyrase inhibition blocks the introduction of negative supercoils, increased expression levels of *gyrAB* and a decreased expression level of *topA* upon Gip overproduction are most probably used to counteract gyrase inhibition. The adaptation at the level of gene expression could then explain the resumed growth of the *gip* expressing strain—reaching almost wild type-like growth rates after a pronounced lag phase (Figure 1).

In summary, we identified Gip as a novel gyrase inhibitor protein encoded by the CGP3 prophage of *C. glutamicum*. Gip was shown to specifically inhibit the gyrase of its bacterial host *C. glutamicum*, but further studies are required to decipher its impact on the phage life cycle.

4 | EXPERIMENTAL PROCEDURES

4.1 | Bacterial strains and growth conditions

All bacterial strains and plasmids used in this study are listed in Tables S1 and S2, respectively. *Corynebacterium glutamicum* ATCC 13032 (NCBI reference: NC_003450.3) was used as a wild-type strain (Ikeda & Nakagawa, 2003). For growth studies and fluorescence measurements as well as for transcriptome analysis, *C. glutamicum* cells were precultivated in BHI (brain heart infusion, Difco BHI, BD, Heidelberg, Germany) at 30°C for 8 hr. The preculture was used to inoculate an overnight culture in CGXII minimal medium with 2% (w/v) glucose (Keilhauer et al., 1993), which was cultivated under

the same conditions. The next day, the overnight culture was used to inoculate the main culture in CGXII minimal medium with 2% (w/v) glucose to an OD_{600} of 1. All media contained kanamycin in a concentration of 25 μg/ml. Gene expression was induced using 50 μM IPTG (Isopropyl β-D-1-thiogalactopyranoside). For standard cloning applications, *E. coli* DH5α was cultivated in Lysogeny Broth (Difco LB, BD, Heidelberg, Germany) medium containing 50 μg/ml kanamycin (LB Kan_{50}) at 37°C and 170 rpm. For protein overproduction and following purification, the *E. coli* BL21 (DE3) strain was used. Precultivation was performed in LB Kan_{50} medium, which was incubated overnight at 37°C and 120 rpm. The main culture was inoculated in LB Kan_{50} medium to an OD_{600} of 0.1 using the pre-culture. At an OD_{600} of 0.6 gene expression was induced using 100 μM IPTG. Cells were harvested after additional 24 hr incubation at 16°C.

4.2 | Recombinant DNA work and cloning techniques

All plasmids and oligonucleotides used in this study are listed in Tables S2 and S3, respectively. Standard cloning techniques like PCR and restriction digestion were performed according to standard protocols (Sambrook & Russell, 2001). In all cases, Gibson assembly was used for plasmid construction (Gibson, 2011). DNA regions of interest were amplified via PCR using the chromosomal DNA of *C. glutamicum* ATCC 13032 as a template. The plasmid backbone was cut using the indicated restriction enzymes. Sequencing and synthesis of oligonucleotides were performed by Eurofins Genomics (Ebersberg, Germany). Genomic deletions were constructed using the pK19*mobsacB* plasmid and the two-step homologs recombination method (Niebisch & Bott, 2001). The 500 bp up- and downstream regions of the respective gene were amplified using the oligonucleotides listed in Table S3. Both PCR products and the digested pK19*mobsacB* plasmid (with HindIII, EcoRI) were assembled via Gibson assembly (Gibson, 2011). The correct deletion was verified by sequencing of the colony PCR product with the indicated oligonucleotides (Table S3).

4.3 | Microtiter cultivation and reporter assays

For growth experiments and fluorescence assays, the BioLector® microcultivation system of m2p-labs (Aachen, Germany) was used (Kensy et al., 2009). The main cultivation was executed in FlowerPlates (MTP-48-B, m2p-labs) at 30°C and 1,200 rpm with a starting OD_{600} of 1 using 750 μl of CGXII minimal media with 2% (w/v) glucose containing 50 μM IPTG and 25 μg/ml kanamycin. During cultivation, biomass was measured as a function of backscattered light intensity with an excitation wavelength of 620 nm (filter module: $\lambda_{Ex}/\lambda_{Em}$: 620 nm/620 nm, gain: 15). Data for biomass measurements were baseline-corrected by subtracting the t_0 value from all data points. The measurements of backscatter were taken at 15 min intervals.

4.4 | Protein purification via affinity tags

For heterologous protein overproduction, *E. coli* BL21 (DE3) cells containing the pET-cg1978-C-*strep* plasmid, the pET-*gyrA*-C-*strep* plasmid, the pET-*gyrA*-N-*strep* plasmid, the pET-*gyrB*-N-*strep* plasmid, or the pET-cg1978-C-*his* plasmid were cultivated as described in "Bacterial strains and growth conditions."

Cell harvesting and disruption were performed as described by Pfeifer et al. (2016). In case of Cg1978-C-Strep, buffer A (100 mM Tris-HCl, pH 8.0) with cOmplete™ Protease inhibitor (Roche, Basel, Switzerland) was used for cell disruption and buffer B (100 mM Tris-HCl, 250 mM NaCl, pH 8.0) for purification. Purification of Strep-tagged Cg1978 was conducted by applying the supernatant to an equilibrated 2 ml Strep-Tactin®-Sepharose® column (IBA, Göttingen, Germany). After washing with 20 ml buffer B, the protein was eluted with 6 ml buffer B containing 15 mM d-desthiobiotin (Sigma–Aldrich, St. Louis, MO, USA). Purification of GyrA-C-Strep, GyrA-N-Strep, and GyrB-N-Strep was conducted in the same way using an adjusted buffer B_{gyr} for cell disruption and purification (buffer B_{gyr}: 20 mM Tris–HCl, 500 mM NaCl, 10% (w/v) glycerol, 5 mM EDTA, 1 mM DTT, pH 7.9).

For purification of Cg1978-C-His, the cell pellet was resuspended in 50 ml TNI20 buffer (20 mM Tris–HCl, 300 mM NaCl, 20 mM imidazole, and pH 8.0) with cOmplete™ Protease inhibitor (Roche, Basel, Switzerland), and cells were disrupted as described above. Purification of His-tagged Cg1978 was performed by applying the supernatant to an equilibrated 2 ml Ni-NTA Agarose column (Invitrogen, California, USA). After washing with 30 ml TNI20 buffer, the protein was eluted with increasing imidazole concentrations using TNI buffer (20 mM Tris–HCl, 300 mM NaCl, pH 8.0) containing 50 mM, 100 mM, 200 mM, or 400 mM imidazole.

After purification, the elution fractions with the highest protein concentration were pooled and analyzed with SDS-PAGE (Laemmli, 1970) using a 4%–20% Mini-PROTEAN® gradient gel (Bio-Rad, Munich, Germany).

4.5 | In vitro pull-down assay and MALDI-TOF analysis

Protein purification of Cg1978-C-Strep was conducted as described above. The elution fractions showing the highest protein concentration in a Bradford assay (Bradford, 1976) were pooled and purified with size-exclusion chromatography using PD10 desalting columns (GE Healthcare, Freiburg, Germany) and buffer B (100 mM Tris–HCl, 250 mM NaCl, pH 8.0) according to manufacturer's manual to remove excess desthiobiotin. For the detection of possible interaction partners of the target protein on a protein-protein level, *C. glutamicum* ATCC 13032 wild-type cells were cultivated in a BHI medium. At an OD_{600} of 5 to 6, the cells were harvested at 11,325 *g* and 4°C for 15 min and cell pellet of 100 ml cell culture was resuspended in 25 ml buffer A (100 mM Tris-HCl, pH 8.0) with cOmplete™ Protease inhibitor (Roche, Basel, Switzerland). Cell disruption was performed using the French Press cell with a pressure of 172 mPA for five passages followed by a centrifugation step at 5,000 *g* for 50 min.

For copurification of possible protein interaction partners, the purified target protein Cg1978 was incubated with the *C. glutamicum* crude extract at RT for 1 hr. After loading the mixture to the StrepTactin column, the purification was performed as described above. The elution fractions with the highest protein concentration were precipitated by the addition of 100% (w/v) trichloroacetic acid (TCA) in a volume ratio of four units of protein to one unit TCA (Sivaraman et al., 1997). After incubation at 4°C overnight, the precipitation approach was centrifuged for 5 min at 14,000 *g*. The supernatant was discarded and the pellet was washed with 200 µl cold acetone twice. Afterward, the pellet was dried for 10 min at 95°C and resuspended in 30 µl 1.5 × SDS loading buffer for gel electrophoresis or in 30 µl trypsin reaction buffer provided by the Trypsin Singles, Proteomics Grade kit (Sigma-Aldrich) for LC-MS/MS sample preparation. Analysis of elution fractions via SDS-PAGE (Laemmli, 1970) was performed using a 4%–20% Mini-PROTEAN® gradient gel (Bio-Rad, Munich, Germany). After staining the gel with Coomassie dye-based RAPIDstain solution (G-Biosciences, St. Louis, MO, USA) MALDI-TOF-MS measurements were performed with an Ultraflex III TOF/TOF mass spectrometer (Bruker Daltonics, Bremen, Germany) for identification of the co-purified proteins (Bussmann et al., 2010). Elution fractions were further analyzed via LC-MS/MS.

4.6 | LC-MS/MS sample preparation and measurement

LC-MS/MS was performed after TCA precipitation using the Trypsin Singles, Proteomics Grade kit (Sigma–Aldrich, St.Louis, MO, USA) according to the manufacturer's instruction. The prepared tryptic peptide samples were separated chromatographically on a nanoLC Eksigent ekspert™ 425 LC system in microLC modus (Sciex) coupled with a 25 Micron ESI Electrode to a TripleTof™ 6600 mass spectrometer (Sciex). As a trap, a YMC-Triart C18 column with the dimension 5 × 0.5 mm ID, 3 µm, 12 nm (YMC) was used, combined with a YMC-Triart C18 column with 150 × 0.3 mm ID, 12 nm, S-3 µm (YMC) as an analytical column. The column oven was set to 40°C.

For trapping, 2% acetonitrile in dd.H_2O with 0.5% formic acid served as a loading solvent, whereas 0.1% formic acid was used as mobile phase A and acetonitrile with 0.1% formic acid (both LC-MS grade, ROTISOLV®, ≥99.9%, Carl Roth) as mobile phase B. First, 10 µl of each sample containing up to 8 µg of digested protein was loaded from the cooled autosampler onto the trap column using 100% loading solvent for 10 min at 10 µl/min for desalting and enrichment.

For the following separation of the peptides on the analytical column, a linear gradient with increasing concentrations of mobile phase B was used starting with 97% A and 3% B and a flow rate of 5 µl/min as an initial condition. During Information-Dependent Acquisition (IDA) and SWATH measurements, the following source and gas settings were applied: 5,500 V spray voltage, 35 psi curtain gas, 12 psi ion source gas 1, 20 psi ion source gas 2, and 150°C interface heater. Each sample was injected three times.

For shotgun measurements, the mass spectrometer was operated with a "top 50" method: Initially, a 250-ms survey scan (TOF-MS mass range *m/z* 400–1,500, high-resolution mode) was collected from which the top 50 precursor ions were automatically selected for fragmentation, whereby each MS/MS 97 Appendix event (mass range *m/z* 170–1,500, in high-sensitivity mode) consisted of a 40 ms fragment ion scan. For parent ion selection, the precursor ion intensity served as the main selection criterion. Ions with an intensity exceeding 100 counts/s and with a charge state of 2+ to 5+ were preferentially selected. Selected precursors were added to a dynamic exclusion list for 22 s and subsequently isolated using a quadrupole resolution of 0.7 amu and fragmented in the collision cell with a rolling collision energy (CE) of 10 eV. If <50 precursor ions fulfilling the selection criteria were detected per survey scan, the detected precursors were subjected to extended MS/MS accumulation time to maintain a constant total cycle time of 2.3 s.

For data analysis, the IDA data were processed with ProteinPilot™ (V5.01, Sciex, USA) using the ParagonTM Algorithm for peptide identification and the ProGroup™ Algorithm for protein identification.

4.7 | DNA microarrays

For a comparative transcriptome analysis of *C. glutamicum* ATCC 13032 carrying the empty pAN6 vector and cells carrying the pAN6-cg1978 vector, cultivation was performed as described in "Bacterial strains and growth conditions" using CGXII-Kan_{25} minimal media with 2% (w/v) glucose and 50 µM IPTG. For both strains, cells were harvested at an OD_{600} of 6 in a reaction tube filled with ice (50 ml) for 5 min at 5,000 *g* and 4°C. RNA purification was carried out using the "RNeasy Mini"-Kit (QIAGEN, Hilden, Germany) according to the manufacturer's manual. The preparation of labeled cDNA and DNA microarray analysis was performed as described previously (Donovan et al., 2015). The data processing was executed with in-house software according to (Polen & Wendisch, 2004). Genes with an mRNA ratio (sample/neg. control) of >2.0 (*p*-value <0.05) were classified as upregulated, whereas genes with an mRNA ratio of <0.5 (*p*-value <0.05) were classified as downregulated. Array data were deposited in the GEO database (ncbi.nlm.nih.gov/geo) with accession number GSE151224.

4.8 | Flow cytometry

Analysis of fluorescent reporter outputs at the single-cell level was performed using the BD Accuri™ C6 flow cytometer (BD biosciences, Heidelberg, Germany). The chromophore of the yellow fluorescent protein eYFP or Venus was excited with a blue laser with an excitation wavelength of 488 nm. The fluorescence emission of eYFP and Venus was measured using a 530/30 nm standard filter. Particle size was detected using the forward light scatter (FSC). The flow cytometer was started up by flushing with filtered, dd.H_2O for 10 min. For preparing flow cytometry samples, cell cultures were mixed with 1 ml flow cytometric fluid (BD™ 342003

FACSFlow™ Sheath Fluid). For every sample, 100,000 events were analyzed via BD Accuri C6 software (version 1.0.264.21).

4.9 | Cultivation and perfusion in microfluidic device

Single-cell analysis of cg1978 overexpressing cells was performed using an in-house developed microfluidic platform (Grünberger et al., 2013, 2015; Helfrich et al., 2015). Cultivation and time-lapse imaging were performed in CGXII minimal medium with 2% (w/v) glucose and 25 μg/ml kanamycin as described by (Pfeifer et al., 2016). Overexpression of cg1978 in the prophage reporter strain ATCC 13032::P_{lys}-*eyfp* carrying the pAN6-cg1978 vector was induced by adding 50 μM IPTG to the medium. An uninduced control served as a reference.

4.10 | Supercoiling inhibition assay

For the supercoiling inhibition assay, Cg1978 as well as both gyrase subunits (GyrA and GyrB) were purified by the means of a C-terminal His-Tag for Cg1978, a C-terminal Strep-Tag for GyrA, and an N-terminal Strep-Tag for GyrB as described above. Using PD10 desalting columns (GE Healthcare, Freiburg, Germany), the buffer of Cg1978 was exchanged to PBS (137 mM NaCl, 2.7 mM KCl, 8 mM Na_2HPO_4, 1.5 mM KH_2PO_4, pH 7.4). In case of GyrA and GyrB, the buffer was exchanged to 20 mM Tris-HCl, pH 7.9, 50% (w/v) glycerol, 0.5 M KCl, and 1 mM DTT. Formation of the heterotetramic gyrase complex was obtained by incubating equimolar amounts of GyrA and GyrB for 30 min on ice. The activity of the purified *C. glutamicum* (*C.g.*) gyrase as well as its inhibition by Cg1978 were determined using the *M. tuberculosis* Gyrase (HIS) Supercoiling Assay Kit (Inspiralis, Norwich, UK) according to the manufacturer's manual. According to the assay conditions, the *C.g.* gyrase concentration of 50 nM resulting in full supercoiling of 0.5 μg relaxed plasmid DNA after 30 min of incubation at 37°C was determined as 1 U. Supercoiling inhibition of the *C.g.* gyrase was assayed by using 1 U of the *C.g.* gyrase with increasing concentrations of Cg1978-C-His (0.02–60.0 μM). Additionally, different concentrations of the known inhibitor ciprofloxacin (10 and 50 μM) were used as a positive control.

Moreover, the inhibitory effect of Cg1978 on the *M.tb* and *E.c.* gyrase was investigated according to the *M. tuberculosis* and *E. coli* Gyrase (HIS) Supercoiling Assay Kits (Inspiralis, Norwich, UK) using 1 U of the respective gyrases and the same Cg1978 concentrations as for the *C.g.* gyrase. All reactions were stopped by adding 30 μl STEB buffer (40% (w/v) sucrose, 100 mM Tris-HCl pH 8.0, 10 mM EDTA, 0.5 mg/ml Bromophenol Blue), and 30 μl chloroform/isoamyl alcohol (v:v, 24:1).

4.11 | Surface Plasmon Resonance Spectroscopy (SPR)

For SPR analysis, Cg1978-C-His and GyrA-N-Strep were purified as described above. After purification, the buffer of both proteins was exchanged to PBS (137 mM NaCl, 2.7 mM KCl, 8 mM Na_2HPO_4, 1.5 mM KH_2PO_4, pH 7.4) using PD10 Desalting columns (GE Healthcare, Freiburg, Germany). The binding of His-tagged Cg1978-C-His to GyrA-N-Strep was analyzed by SPR analysis in a Biacore 3000 device (GE Healthcare, Freiburg, Germany) using a Sensor Chip CM5 (GE Healthcare, Freiburg, Germany). As the first step, an anti-histidine antibody (GE Healthcare, Freiburg, Germany) was immobilized to the chip matrix using amino coupling chemistry. All experiments were carried out in HBS-EP buffer (0.01 M HEPES, pH 7.4, 0.15 M NaCl, 3 mM EDTA, 0.005% v/v Surfactant P20) at 25°C. Following the standard coupling protocol for antibody immobilization, the mixture of 0.05 M N-Hydroxysuccinimide (NHS) and 0.2 M 1-Ethyl-3-(3-dimethylamino propyl) carbodiimide hydrochloride (EDC) was injected for a total contact time of 420 s to activate the matrix. Then, the anti-histidine antibody (50 μg/ml) diluted in immobilization buffer (10 mM sodium acetate, pH 4.5) was injected for 420 s. To deactivate the unbound parts of the chip matrix, 1 M ethanolamine hydrochloride-NaOH (pH 8.5) was injected for 420 s. The flow rate was set to 10 μl/min during this immobilization procedure. Approximately 8.000–10.000 response units (RU) of the anti-histidine antibody were immobilized per flow cell. For the binding analysis, 180–250 RU of Cg1978-C-His was captured via injection of 40 μl (10 nM) at a flow rate of 5 μl/min followed by 10 min of HBS-EP buffer to remove unbound protein from the chip. The binding analysis between Cg1978-C-His and GyrA-N-Strep was then performed by injecting 90 μl of GyrA-N-Strep (10–250 nM) followed by a dissociation time of 300 s at a flow rate of 30 μl/min. After each cycle, the surface was regenerated by injection of regeneration buffer (10 mM Glycine-HCl, pH 1.5) for 30 s, at a flow rate of 30 μl/min. After the equilibration with three start up cycles without the analyte, this was repeated for various concentrations of GyrA-N-Strep (10–250 nM). Sensorgrams were recorded using Biacore 3000 Control Software 4.1.2 and analyzed with BIAevaluation software 4.1.1 (GE Healthcare, Freiburg, Germany). The surface of flow cell 1 immobilized with the anti-histidine antibody was used to obtain blank sensorgrams for the subtraction of the bulk refractive index background. The referenced sensorgrams were normalized to a baseline of 0. Peaks in the sensorgrams at the beginning and the end of the injection are due to the run-time difference between the flow cells for the chip.

ACKNOWLEDGMENTS

We thank the European Research Council (ERC Starting Grant, grant number 757563) and the Helmholtz Association (grant number W2/W3-096) for financial support. We thank Astrid Wirtz for technical assistance with respect to the LC-MS/MS measurement. We thank Rebecca Lukaschewsky for constructing the gyrase overexpression plasmids. SPR analyses were performed in the Bioanalytics service unit of the JGU Biocenter. We very much thank the reviewers of this manuscript for their critical but constructive comments during the review process. Open access funding enabled and organized by ProjektDEAL.

CONFLICT OF INTEREST

The authors declare no conflict of interest.

AUTHOR CONTRIBUTIONS

LK, MH, and JF conceived the study; LK and JB performed the experiments; LK, MH, JB, RH, and JF analyzed the data; LK and JF wrote the manuscript. All authors reviewed and edited the manuscript.

DATA AVAILABILITY STATEMENT

The data that support the findings of this study are available in the supplementary material of this article. Microarray data were deposited in the GEO database (ncbi.nlm.nih.gov/geo) with accession number GSE151224.

ORCID

Julia Frunzke https://orcid.org/0000-0001-6209-7950

REFERENCES

Ahmed, W., Menon, S., Karthik, P.V. & Nagaraja, V. (2016) Autoregulation of topoisomerase I expression by supercoiling sensitive transcription. *Nucleic Acids Research*, *44*(4), 1541–1552. https://doi.org/10.1093/nar/gkv1088

Bernard, P., Kézdy, K.E., Van Melderen, L., Steyaert, J., Wyns, L., Pato, M.L. et al. (1993) The F plasmid CcdB protein induces efficient ATP-dependent DNA cleavage by gyrase. *Journal of Molecular Biology*, *234*(3), 534–541. https://doi.org/10.1006/jmbi.1993.1609

Bradford, M.M. (1976) A rapid and sensitive method for the quantitation of microgram quantities of protein utilizing the principle of protein-dye binding. *Analytical Biochemistry*, *72*, 248–254. https://doi.org/10.1006/abio.1976.9999

Bush, N.G., Evans-Roberts, K. & Maxwell, A. (2015) DNA topoisomerases. *EcoSal Plus*, *6*(2), https://doi.org/10.1128/ecosalplus.ESP-0010-2014

Bussmann, M., Baumgart, M. & Bott, M. (2010) RosR (Cg1324), a hydrogen peroxide-sensitive MarR-type transcriptional regulator of *Corynebacterium glutamicum*. *Journal of Biological Chemistry*, *285*(38), 29305–29318. https://doi.org/10.1074/jbc.M110.156372

Chatterji, M., Unniraman, S., Mahadevan, S. & Nagaraja, V. (2001) Effect of different classes of inhibitors on DNA gyrase from *Mycobacterium smegmatis*. *Journal of Antimicrobial Chemotherapy*, *48*(4), 479–485. https://doi.org/10.1093/jac/48.4.479

Collin, F., Karkare, S. & Maxwell, A. (2011) Exploiting bacterial DNA gyrase as a drug target: current state and perspectives. *Applied Microbiology and Biotechnology*, *92*(3), 479–497. https://doi.org/10.1007/s00253-011-3557-z

Dao-Thi, M.H., Van Melderen, L., De Genst, E., Afif, H., Buts, L., Wyns, L. et al. (2005) Molecular basis of gyrase poisoning by the addiction toxin CcdB. *Journal of Molecular Biology*, *348*(5), 1091–1102. https://doi.org/10.1016/j.jmb.2005.03.049

De Smet, J., Hendrix, H., Blasdel, B.G., Danis-Wlodarczyk, K. & Lavigne, R. (2017) *Pseudomonas* predators: understanding and exploiting phage-host interactions. *Nature Reviews Microbiology*, *15*(9), 517–530. https://doi.org/10.1038/nrmicro.2017.61

De Smet, J., Wagemans, J., Boon, M., Ceyssens, P.-J., Voet, M., Noben, J.-P. et al. (2021) The bacteriophage LUZ24 "Igy" peptide inhibits the *Pseudomonas* DNA gyrase. *Cell Reports*, *36*(8), 109567. https://doi.org/10.1016/j.celrep.2021.109567

DeMarini, D.M. & Lawrence, B.K. (1992) Prophage induction by DNA topoisomerase II poisons and reactive-oxygen species: role of DNA breaks. *Mutation Research*, *267*(1), 1–17. https://doi.org/10.1016/0027-5107(92)90106-C

Ding, Y., Manzo, C., Fulcrand, G., Leng, F., Dunlap, D. & Finzi, L. (2014) DNA supercoiling: a regulatory signal for the λ repressor. *Proceedings of the National Academy of Sciences of the United States of America*, *111*(43), 15402–15407. https://doi.org/10.1073/pnas.1320644111

Donovan, C., Heyer, A., Pfeifer, E., Polen, T., Wittmann, A., Krämer, R. et al. (2015) A prophage-encoded actin-like protein required for efficient viral DNA replication in bacteria. *Nucleic Acids Research*, *43*(10), 5002–5016. https://doi.org/10.1093/nar/gkv374

Dorman, C.J. & Dorman, M.J. (2016) DNA supercoiling is a fundamental regulatory principle in the control of bacterial gene expression. *Biophysical Reviews*, *8*(3), 209–220. https://doi.org/10.1007/s12551-016-0205-y

Drlica, K. & Malik, M. (2003) Fluoroquinolones: action and resistance. *Current Topics in Medicinal Chemistry*, *3*(3), 249–282. https://doi.org/10.2174/1568026033452537

Dwyer, D.J., Kohanski, M.A., Hayete, B. & Collins, J.J. (2007) Gyrase inhibitors induce an oxidative damage cellular death pathway in *Escherichia coli*. *Molecular Systems Biology*, *3*, 91. https://doi.org/10.1038/msb4100135

Frunzke, J., Bramkamp, M., Schweitzer, J.E. & Bott, M. (2008) Population Heterogeneity in *Corynebacterium glutamicum* ATCC 13032 caused by prophage CGP3. *Journal of Bacteriology*, *190*(14), 5111–5119. https://doi.org/10.1128/JB.00310-08

Gibson, D.G. (2011) Enzymatic assembly of overlapping DNA fragments. *Methods in Enzymology*, *498*, 349–361. https://doi.org/10.1016/B978-0-12-385120-8.00015-2

Grünberger, A., Probst, C., Helfrich, S., Nanda, A., Stute, B., Wiechert, W. et al. (2015) Spatiotemporal microbial single-cell analysis using a high-throughput microfluidics cultivation platform. *Cytometry Part A*, *87*(12), 1101–1115. https://doi.org/10.1002/cyto.a.22779

Grünberger, A., van Ooyen, J., Paczia, N., Rohe, P., Schiendzielorz, G., Eggeling, L. et al. (2013) Beyond growth rate 0.6: *Corynebacterium glutamicum* cultivated in highly diluted environments. *Biotechnology and Bioengineering*, *110*(1), 220–228. https://doi.org/10.1002/bit.24616

Guha, S., Udupa, S., Ahmed, W. & Nagaraja, V. (2018) Rewired down-regulation of DNA gyrase impacts cell division, expression of topology modulators, and transcription in *Mycobacterium smegmatis*. *Journal of Molecular Biology*, *430*(24), 4986–5001. https://doi.org/10.1016/j.jmb.2018.10.001

Hatfull, G.F. (2015) Dark matter of the biosphere: the amazing world of bacteriophage diversity. *Journal of Virology*, *89*(16), 8107–8110. https://doi.org/10.1128/jvi.01340-15

Helfrich, S., Pfeifer, E., Krämer, C., Sachs, C.C., Wiechert, W., Kohlheyer, D. et al. (2015) Live cell imaging of SOS and prophage dynamics in isogenic bacterial populations. *Molecular Microbiology*, *98*(4), 636–650. https://doi.org/10.1111/mmi.13147

Ikeda, M. & Nakagawa, S. (2003) The *Corynebacterium glutamicum* genome: features and impacts on biotechnological processes. *Applied Microbiology and Biotechnology*, *62*(2–3), 99–109. https://doi.org/10.1007/s00253-003-1328-1

Janion, C. (2008) Inducible SOS response system of DNA repair and mutagenesis in *Escherichia coli*. *International Journal of Biological Sciences*, *4*(6), 338–344. https://doi.org/10.7150/ijbs.4.338

Jeong, K.S., Xie, Y., Hiasa, H. & Khodursky, A.B. (2006) Analysis of pleiotropic transcriptional profiles: a case study of DNA gyrase inhibition. *PLoS Genetics*, *2*(9), e152. https://doi.org/10.1371/journal.pgen.0020152

Keilhauer, C., Eggeling, L. & Sahm, H. (1993) Isoleucine synthesis in *Corynebacterium glutamicum*: molecular analysis of the *ilvB-ilvN-ilvC* operon. *Journal of Bacteriology*, *175*(17), 5595–5603. https://doi.org/10.1128/jb.175.17.5595-5603.1993

Kensy, F., Zang, E., Faulhammer, C., Tan, R.K. & Büchs, J. (2009) Validation of a high-throughput fermentation system based on online monitoring of biomass and fluorescence in continuously shaken microtiter plates. *Microbial Cell Factories*, *8*, 31. https://doi.org/10.1186/1475-2859-8-31

Laemmli, U.K. (1970) Cleavage of structural proteins during assembly of head of bacteriophage T4. *Nature*, *227*(5259), 680–685. https://doi.org/10.1038/227680a0

Lu, S., Wang, J., Chitsaz, F., Derbyshire, M.K., Geer, R.C., Gonzales, N.R. et al. (2020) CDD/SPARCLE: the conserved domain database in 2020. *Nucleic Acids Research*, *48*(D1), D265–D268. https://doi.org/10.1093/nar/gkz991

Madhusudan, K. & Nagaraja, V. (1996) Alignment and phylogenetic analysis of type II DNA topoisomerases. *Journal of Biosciences*, *21*, 613–629. https://doi.org/10.1007/BF02703140

Manjunatha, U.H., Dalal, M., Chatterji, M., Radha, D.R., Visweswariah, S.S. & Nagaraja, V. (2002) Functional characterisation of mycobacterial DNA gyrase: an efficient decatenase. *Nucleic Acids Research*, *30*(10), 2144–2153. https://doi.org/10.1093/nar/30.10.2144

Manjunatha, U.H., Madhusudan, K., Visweswariah, S. & Nagaraja, V. (2000) Structural heterogeneity in DNA gyrases in Gram-positive and Gram-negative bacteria. *Current Science*, *79*(7), 968–974.

Mattenberger, Y., Silva, F. & Belin, D. (2015) 55.2, a phage T4 ORFan gene, encodes an inhibitor of *Escherichia coli* topoisomerase I and increases phage fitness. *PLoS One*, *10*(4), e0124309. https://doi.org/10.1371/journal.pone.0124309

Maxwell, A. & Lawson, D.M. (2003) The ATP-binding site of type II topoisomerases as a target for antibacterial drugs. *Current Topics in Medicinal Chemistry*, *3*(3), 283–303. https://doi.org/10.2174/1568026033452500

McKie, S.J., Neuman, K.C. & Maxwell, A. (2021) DNA topoisomerases: advances in understanding of cellular roles and multi-protein complexes via structure-function analysis. *BioEssays*, *43*(4), e2000286. https://doi.org/10.1002/bies.202000286

Menzel, R. & Gellert, M. (1983) Regulation of the genes for *E. coli* DNA gyrase: homeostatic control of DNA supercoiling. *Cell*, *34*, 105–113. https://doi.org/10.1016/0092-8674(83)90140-X

Miki, T., Park, J.A., Nagao, K., Murayama, N. & Horiuchi, T. (1992) Control of segregation of chromosomal DNA by sex factor F in *Escherichia coli*. Mutants of DNA gyrase subunit A suppress *letD (ccdB)* product growth inhibition. *Journal of Molecular Biology*, *225*(1), 39–52. https://doi.org/10.1016/0022-2836(92)91024-j

Nanda, A.M., Heyer, A., Krämer, C., Grünberger, A., Kohlheyer, D. & Frunzke, J. (2014) Analysis of SOS-induced spontaneous prophage induction in *Corynebacterium glutamicum* at the single-cell level. *Journal of Bacteriology*, *196*(1), 180–188. https://doi.org/10.1128/JB.01018-13

Niebisch, A. & Bott, M. (2001) Molecular analysis of the cytochrome bc_1-aa_3 branch of the *Corynebacterium glutamicum* respiratory chain containing an unusual diheme cytochrome c_1. *Archives of Microbiology*, *175*(4), 282–294. https://doi.org/10.1007/s002030100262

Nobrega, F.L., Vlot, M., de Jonge, P.A., Dreesens, L.L., Beaumont, H.J.E., Lavigne, R. et al. (2018) Targeting mechanisms of tailed bacteriophages. *Nature Reviews Microbiology*, *16*(12), 760–773. https://doi.org/10.1038/s41579-018-0070-8

Norregaard, K., Andersson, M., Sneppen, K., Nielsen, P.E., Brown, S. & Oddershede, L.B. (2013) DNA supercoiling enhances cooperativity and efficiency of an epigenetic switch. *Proceedings of the National Academy of Sciences of the United States of America*, *110*(43), 17386–17391. https://doi.org/10.1073/pnas.1215907110

Norregaard, K., Andersson, M., Sneppen, K., Nielsen, P.E., Brown, S. & Oddershede, L.B. (2014) Effect of supercoiling on the λ switch. *Bacteriophage*, *4*(1), e27517. https://doi.org/10.4161/bact.27517

Ofir, G. & Sorek, R. (2018) Contemporary phage biology: from classic models to new insights. *Cell*, *172*(6), 1260–1270. https://doi.org/10.1016/j.cell.2017.10.045

Orr, M.W., Mao, Y., Storz, G. & Qian, S.B. (2020) Alternative ORFs and small ORFs: shedding light on the dark proteome. *Nucleic Acids Research*, *48*(3), 1029–1042. https://doi.org/10.1093/nar/gkz734

Pfeifer, E., Hünnefeld, M., Popa, O., Polen, T., Kohlheyer, D., Baumgart, M. et al. (2016) Silencing of cryptic prophages in *Corynebacterium glutamicum*. *Nucleic Acids Research*, *44*(21), 10117–10131. https://doi.org/10.1093/nar/gkw692

Pierrat, O.A. & Maxwell, A. (2003) The action of the bacterial toxin microcin B17. *Journal of Biological Chemistry*, *278*(37), 35016–35023. https://doi.org/10.1074/jbc.M304516200

Polen, T. & Wendisch, V.F. (2004) Genomewide expression analysis in amino acid-producing bacteria using DNA microarrays. *Applied Biochemistry and Biotechnology*, *118*, 215–232. https://doi.org/10.1385/ABAB:118:1-3:215

Roach, D.R. & Donovan, D.M. (2015) Antimicrobial bacteriophage-derived proteins and therapeutic applications. *Bacteriophage*, *5*(3), e1062590. https://doi.org/10.1080/21597081.2015.1062590

Rohwer, F. & Youle, M. (2011) Consider something viral in your search. *Nature Reviews Microbiology*, *9*(5), 308–309. https://doi.org/10.1038/nrmicro2563

Sambrook, J. & Russell, D.W. (2001) *Molecular cloning: a laboratory manual*, 3rd edition. Cold Spring Harbor Laboratory Press.

Schroven, K., Aertsen, A. & Lavigne, R. (2021) Bacteriophages as drivers of bacterial virulence and their potential for biotechnological exploitation. *FEMS Microbiology Reviews*, *45*(1), fuaa041. https://doi.org/10.1093/femsre/fuaa041

Shah, S. & Heddle, J.G. (2014) Squaring up to DNA: pentapeptide repeat proteins and DNA mimicry. *Applied Microbiology and Biotechnology*, *98*(23), 9545–9560. https://doi.org/10.1007/s00253-014-6151-3

Sivaraman, T., Kumar, T.K.S., Jayaraman, G. & Yu, C. (1997) The mechanism of 2,2,2-trichloroacetic acid-induced protein precipitation. *Journal of Protein Chemistry*, *16*(4), 291–297. https://doi.org/10.1023/A:1026357009886

Storz, G., Wolf, Y.I. & Ramamurthi, K.S. (2014) Small proteins can no longer be ignored. *Annual Review of Biochemistry*, *83*, 753–777. https://doi.org/10.1146/annurev-biochem-070611-102400

Tomasz, M. (1995) Mitomycin C: small, fast and deadly (but very selective). *Chemistry and Biology*, *2*(9), 575–579. https://doi.org/10.1016/1074-5521(95)90120-5

Tse-Dinh, Y.-C. (1985) Regulation of the *Escherichia coli* DNA topoisomerase I gene by DNA supercoiling. *Nucleic Acids Research*, *13*(13), 4751–4763. https://doi.org/10.1093/nar/13.13.4751

Vanden Broeck, A., Lotz, C., Ortiz, J. & Lamour, V. (2019) Cryo-EM structure of the complete *E. coli* DNA gyrase nucleoprotein complex. *Nature Communications*, *10*(1), 4935. https://doi.org/10.1038/s41467-019-12914-y

Wendisch, V.F., Jorge, J.M.P., Pérez-García, F. & Sgobba, E. (2016) Updates on industrial production of amino acids using *Corynebacterium glutamicum*. *World Journal of Microbiology and Biotechnology*, *32*(6), 105. https://doi.org/10.1007/s11274-016-2060-1

Wiechert, J., Filipchyk, A., Hünnefeld, M., Gätgens, C., Brehm, J., Heermann, R. et al. (2020). Deciphering the rules underlying xenogeneic silencing and counter-silencing of Lsr2-like proteins using CgpS of *Corynebacterium glutamicum* as a model. *mBio*, *11*(1), e02273-19. https://doi.org/10.1128/mBio.02273-19

Yin, Y. & Fischer, D. (2008) Identification and investigation of ORFans in the viral world. *BMC Genomics*, *9*, 24. https://doi.org/10.1186/1471-2164-9-24

SUPPORTING INFORMATION

Additional supporting information may be found in the online version of the article at the publisher's website.

How to cite this article: Kever, L., Hünnefeld, M., Brehm, J., Heermann, R. & Frunzke, J. (2021) Identification of Gip as a novel phage-encoded gyrase inhibitor protein of *Corynebacterium glutamicum*. *Molecular Microbiology*, 116, 1268–1280. https://doi.org/10.1111/mmi.14813